

Probing dynamics at interfaces: resonance enhanced dynamic light scattering

Markus A. Plum¹, Werner Steffen^{1,*}, George Fytas^{1,2,*}, Wolfgang Knoll^{1,3} and Bernhard Menges¹

¹Max Planck Institute for Polymer Research, P. O. Box 3148, 55128 Mainz, Germany

²Department of Material Science, University of Crete/F.O.R.T.H P.O. Box 1527, 71110 Heraklion, Greece

³Currently with the Austrian Research Centers GMBH – ARC Tech Gate Vienna, 1220 Wien

*steffen@mpip-mainz.mpg.de, fyta@mpip-mainz-mpg.de

Abstract: Experiments addressing supramolecular dynamics at interfaces are of paramount importance for the understanding of the dynamic behaviour of polymers, particles, or cells at interfaces, transport phenomena to and from surfaces, thin films or membranes. However, there are only few reports in the literature due to the paucity of experimental methods that offer the required spatial and time resolution. Evanescent wave dynamic light scattering originally developed to meet these needs has limited sensitivity and is restricted to glass substrates. Here we report the first experimental realization of a dynamic light scattering experiment close to an interface using surface plasmon polaritons as light source offering a strong increase in the signal to noise ratio and allowing for the use of metallic interfaces. As a proof of concept, we consider the diffusion of particles with radii down to 10nm in dilute dispersions close to a gold surface.

© 2006 Optical Society of America

OCIS codes: (240.6648) Surface dynamics; (240.6680) Surface plasmons; (290.1990) Diffusion

References and links

1. S. C. Bae and S. Granick, "Molecular Motion at Soft and Hard Interfaces: From Phospholipid Bilayers to Polymers and Lubricants," *Annu. Rev. Phys. Chem.* **58**, 353-374 (2007).
2. S. A. Sukhishvili, Y. Chen, J. D. Muller, E. Gratton, K. S. Schweizer, and S. Granick, "Materials science: Diffusion of a polymer pancake," *Nature* **406**, 146-146 (2000).
3. K. D. Kihm, A. Banerjee, C. K. Choi, and T. Takagi, "Near-wall hindered Brownian diffusion of nanoparticles examined by three-dimensional ratiometric total internal reflection fluorescence microscopy (3-D R-TIRFM)," *Exp. Fluids* **37**, 811-824 (2004).
4. C. Genet and T. W. Ebbesen, "Light in tiny holes," *Nature* **445**, 39-46 (2007).
5. K. H. Lan, N. Ostrowsky, and D. Sornette, "Brownian dynamics close to a wall studied by photon correlation spectroscopy from an evanescent wave," *Phys. Rev. Lett.* **57**, 17-20 (1986).
6. G. Fytas, S. H. Anastasiadis, R. Seghrouchni, D. Vlassopoulos, J. Li, B. J. Factor, W. Theobald, and C. Toprakcioglu "Probing Collective Motions of Terminally Anchored Polymers," *Science* **274**, 2041-2044 (1996).
7. M. Hosoda, K. Sakai, and K. Takagi, "Measurement of anisotropic Brownian motion near an interface by evanescent light-scattering spectroscopy," *Phys. Rev. E* **58**, 6275-6280 (1998).
8. N. Lin, J. Yu, and S. A. Rice, "Direct measurements of constrained Brownian motion of an isolated sphere between two walls," *Phys. Rev. E* **62**, 3909-3919 (2000).
9. P. Holmqvist, J. Dhont, and P. Lang, "Colloidal dynamics near a wall studied by evanescent wave light scattering: Experimental and theoretical improvements and methodological limitations," *J. Chem. Phys.* **126**, 044707 (2007).
10. V. N. Michailidou, G. Petekidis, J. W. Swan, and J. F. Brady, "Dynamics of Concentrated Hard-Sphere Colloids Near a Wall," *Phys. Rev. Lett.* **102**, 068302 (2009).
11. G. E. Yakubov, B. Loppinet, H. Zhang, J. R  he, R. Sigel, and G. Fytas "Collective Dynamics of an End-Grafted Polymer Brush in Solvents of Varying Quality," *Phys. Rev. Lett.* **92**, 115501 (2004).
12. R. B. M. Schasfoort, and A. J. Tudos, *Handbook of Surface Plasmon Resonance* (RSC Publishing, Cambridge, 2008).
13. W. Knoll, "Interfaces and thin films as seen by bound electromagnetic waves," *Annu. Rev. Phys. Chem.* **49**, 569-638 (1998).

14. J. Homola, "Surface Plasmon Resonance Sensors for Detection of Chemical and Biological Species," *Chem. Rev.* **108**, 462-493 (2008).
 15. A. Baba, M. K. Park, R. C. Advincula, and W. Knoll, "Simultaneous Surface Plasmon Optical and Electrochemical Investigation of Layer-by-Layer Self-Assembled Conducting Ultrathin Polymer Films," *Langmuir* **18**, 4648-4652 (2002).
 16. H. Raether, *Surface plasmons on smooth and rough surfaces and on gratings* (Springer, Berlin, 1988).
 17. W. L. Barnes, A. Dereux, and T. W. Ebbesen, "Surface plasmon subwavelength optics," *Nature* **424**, 824-830 (2003).
 18. E. Kretschmann, and H. Raether "Radiative decay of non radiative surface plasmons excited by light," *Z. Naturforsch.* **23a**, 2135-2136 (1968).
 19. T. Liebermann and W. Knoll, "Surface-plasmon field-enhanced fluorescence spectroscopy," *Colloids Surf. A* **171**, 115-130 (2000).
 20. Y. Naoi and M. Fukui, "Intensity of surface-plasmon polariton energy emitted into the air side in an air/Ag-film/prism configuration," *Phys. Rev. B* **42**, 5009-5012 (1990).
 21. J. Happel and H. Brenner, *Low Reynolds number Hydrodynamics with special applications to particulate media* (Nijhoff, The Hague, 1983), Chap. 7.
 22. S. Ekgasit, A. Tangcharoenbumrungsuk, F. Yu, A. Baba, and W. Knoll, "Resonance shifts in SPR curves of nonabsorbing, weakly absorbing, and strongly absorbing dielectrics," *Sens. Actuators B* **105**, 532-541 (2005)
 23. A. Unger, U. Trutschel, and U. Langbein, "Design software for stratified optical systems with planar and cylindrical symmetry," in *DGaO-Proceedings 2007*, http://www.dgao-proceedings.de/download/108/108_p12.pdf.
 24. WINSPALL is a software which computes the reflectivity of optical multilayer systems. It is based on the fresnel equations and the matrix formalism and can be downloaded from: <http://www.mpip-mainz.mpg.de/knoll/soft/>.
 25. M. J. Joy, P. S. Cann, J. R. Sambles and E. A. Perkins "Surface-plasmon-enhanced light scattering from microscopic spheres," *Appl. Phys. Lett.* **83**, 3006-3008 (2003).
 26. J. Dostálek, Austrian Research Centers GmbH, Nano-System-Technologies TechGate: Donau-City-Straße 1, 1220 Vienna, Austria (personal communication, 2009)
-

1. Introduction

Local structure and properties of materials in the immediate vicinity of a solid surface often differ from those in the bulk state due to physical and chemical influence of the interface [1]. These effects extend into the medium only on length scales of the order of sub micrometres. To monitor physical properties of this near-interface region with spatial and temporal resolution demands for powerful experimental techniques. In the last years correlation spectroscopy analyzing the fluctuation of either fluorescence [2-4] or light scattering intensities in a total internal reflection configuration [5, 6] have been developed in order to extract information on dynamical processes. In the latter technique, the strong localization of the evanescent wave (EW) near the interface combines the spatial resolution of the conventional dynamic laser light scattering (DLS) with the possibility to probe interphases at different distances from the glass surface [7-10]. The main disadvantages of EWDLS are the lack of species selectivity, the restriction to glass substrates and the generally weak signal that limits the potential numerous applications [11]. For example a recent EWDLS study of the particle diffusion near a glass wall has reported a lower size limit of about 30nm radius [9]. To expand into bio-relevant systems, it is expedient to establish a method to probe dynamics for smaller systems, e.g. particle radii smaller than 15nm. Since light scattering intensity I strongly depends on the particle size R ($I \sim R^6$) one requires enormous enhancement factors to be up to the mark. Furthermore the restriction to glass substrates and hence dielectric surfaces excludes the use of metallic films, which are important platforms for electrochemical processes and biosensor applications [12-15].

Here we utilize Surface Plasmon Polaritons [16,17] as incident electromagnetic field instead of the evanescent field generated by total internal reflection in order to boost the signal and to overrule the substrate limitation at the same time. As a proof of concept and to fathom the possibilities of this emerging technique, we address the diffusion of spherical particles with radii from 10nm to 40nm in the dilute concentration regime. High quality experimental relaxation functions were obtained with laser powers of less than milliwatt using a gold/silver

surface and particle number densities of the order of 10^{12}cm^{-3} . Under these conditions, EWDLS can hardly be utilized.

2. Theory

2.1 Surface Plasmon Resonance (SPR)

According to Maxwell theory an electromagnetic surface wave can propagate along the boundary between a dielectric and a metal and behaves like a quasi free electron plasma. The surface plasmon is a transverse-magnetic (TM₀) mode and has the same wavelength and coherence as the exciting laser beam. As a consequence of the energy dissipation of this mode through the metal layer, they are damped in the direction of propagation. Therefore the surface waves have their intensity maximum at the interface metal/dielectric with an exponential decaying field perpendicular to the surrounding media [16].

The condition to excite surface plasmons by light using the Kretschmann-Raether configuration [16,18] is given in the following equation for the incidence angle Ψ :

$$\sin \Psi = \frac{1}{\sqrt{\epsilon_p}} \cdot \sqrt{\frac{\epsilon_m' \cdot \epsilon_d}{\epsilon_m' + \epsilon_d}} \quad (1)$$

where the relative permittivity of the dielectric and the prism are given by ϵ_d and ϵ_p respectively, and ϵ_m' is the real part of the dielectric function ϵ_m of the metal used.

2.2 DLS

DLS is a very powerful method to characterize the dynamics of polymers and nanoparticles in solution. For dilute dispersions of strictly monodisperse spherical particles of radius R undergoing free Brownian motion, the relaxation function $C(q,t)$ for the particle concentration fluctuations with a wave vector q is a single-exponential decay function with a purely diffusive relaxation rate $\Gamma_0=D_0q^2$; the translational diffusion coefficient D_0 relates to the particle radius R and the solvent viscosity η via the Stokes-Einstein relation:

$$D_0 = \frac{k_B T}{6\pi\eta R} \quad (2)$$

with T and k_B being the absolute temperature and Boltzmann's constant, respectively. Deviations of $C(q,t)$ from the exponential shape, which are anticipated in EWDLS[10] can be well described by the stretched exponential function,

$$C(q,t) = \exp\left\{-\left(\Gamma_s \cdot t\right)^\beta\right\} \quad (3)$$

where Γ_s is the characteristic rate of $C(q,t)$ whose integral yields the average rate $\Gamma_{av}=\beta\Gamma_s/\Gamma(1/\beta)$ with Γ being the Gamma function. The shape parameter $0 < \beta < 1$ is a measure of the relaxation rate distribution. An alternative description is the cumulant analysis

$$\ln C(q,t) = -\Gamma_c t + (\mu_2/2)t^2 - \dots \quad (4)$$

that yields the initial decay rate Γ_c and the variance μ_2 of the distribution which contains the gradient of the mobility normal to the interface [9]. It is this short time behavior of $C(q,t)$ that can be computed from theory.

2.3 Resonance Enhanced Dynamic Light Scattering (REDLS)

At $\lambda=632.8\text{nm}$ the resonant excitation of surface plasmons provides an enhancement factor of the square of the evanescent field (intensity) of 16 for gold and up to 80 for silver surfaces as compared to the gain of maximum of 4 in the EWDLS experiment [13,19]. This opens up new possibilities for the study of dynamics close to a solid wall at very low levels of incident laser power for macromolecules and particles at low concentrations. The reported work herein is a

combination of SPR spectroscopy and DLS that introduces a new technique (REDLS) in surface and interface science.

Theoretically, a surface plasmon propagates along the surface of a conductor in contact to a dielectric medium and only light scattered by this wave should be observed. For particles of radius $R=30\text{nm}$ at a concentration of 0.5g/l or 10^5 particles per scattering volume and laser power less than milliwatt, the scattered light intensity would be very weak in spite of the surface plasmon field enhancement.

Even though the surface plasmon is in principle a nonradiative mode it has been shown that it radiates light into all directions [16,20]. The mechanism of this emission has its seeds in the roughness of the surface or inhomogeneities of the dielectric constant inside the plasma [16]. This plasmon radiation and the quasi-elastic light scattering from the particles lead to a heterodyne mixing at the DLS detector (Fig. 1(A)). Under these heterodyne conditions, the measured autocorrelation function $G(q,t)$ is the electric field autocorrelation yielding directly the desired relaxation function $C(q,t)$ - a property of the system. Thus, the improved statistics become apparent from the quality of the experimental $C(q,t)$ as seen in Fig. 1(C). Due to the elastic contribution of the surface plasmon radiation, the experimental intensity correlation functions are recorded under heterodyne conditions and relate therefore directly to the field autocorrelation function $C(q,t)$.

We found that it is extremely important to control the surface roughness of the metallic films used in the experiment, since too strong elastic light contribution diminishes the contrast of $G(q,t)$. It can further affect the q -dependence of $G(q,t)$ since the plasmon radiation can vary the heterodyne conditions.

2.4 Anisotropic diffusion near an interface

The foundation of the theory of diffusion close to a solid wall was laid already some time ago by Faxen and Brenner [21]. A hard sphere with radius R , moving in a fluid of viscosity η experiences a hydrodynamic drag force opposite to its velocity. When the sphere approaches a rigid, immobile, impenetrable and flat surface the drag force is modified leading to an anisotropic hindered diffusion parallel and normal to the surface i.e. $D_{\parallel,\perp}/D_0 \leq 1$. This theory was adopted for EWDLS. Taking into account the hydrodynamic interactions between the spherical particles and the surface as well as the evanescent geometry, the initial relaxation rate Γ_c describing the short time behavior of $C(q,t)$ [Eq. (4)] can be rewritten as:

$$\Gamma_c = Q_{\parallel}^2 D_{\parallel} + \left(Q_{\perp}^2 + \frac{1}{\xi^2} \right) D_{\perp} \quad (5)$$

where $Q_{\parallel,\perp}$ are the magnitude of the q component, $D_{\parallel,\perp}$ are the “mean diffusivities” parallel and perpendicular to the surface and ξ is the penetration depth [9]. Due to the large drag force near the wall both $D_{\parallel,\perp} < D_0$ for $\xi/R < 10$ [9]. The two diffusion coefficients do not include non-hydrodynamic effects such as electrostatic and electro-osmotic forces that maybe exist within the submicrometer range of the evanescent field.

3. REDLS-Setup

The principles and a schematic set-up of the REDLS technique are shown in Fig. 1. SPR spectroscopy is performed in Kretschmann-Raether configuration with a setup as described elsewhere [22]. A DLS geometry is attached to collect the scattered light at selected angles Θ' and hence probing at selected wave vectors \mathbf{q} . The magnitude of the scattering wave vector \mathbf{q} (Fig. 1(A)) is calculated from

$$|\mathbf{q}| = 2k_i \sin(\Theta/2) \quad (6)$$

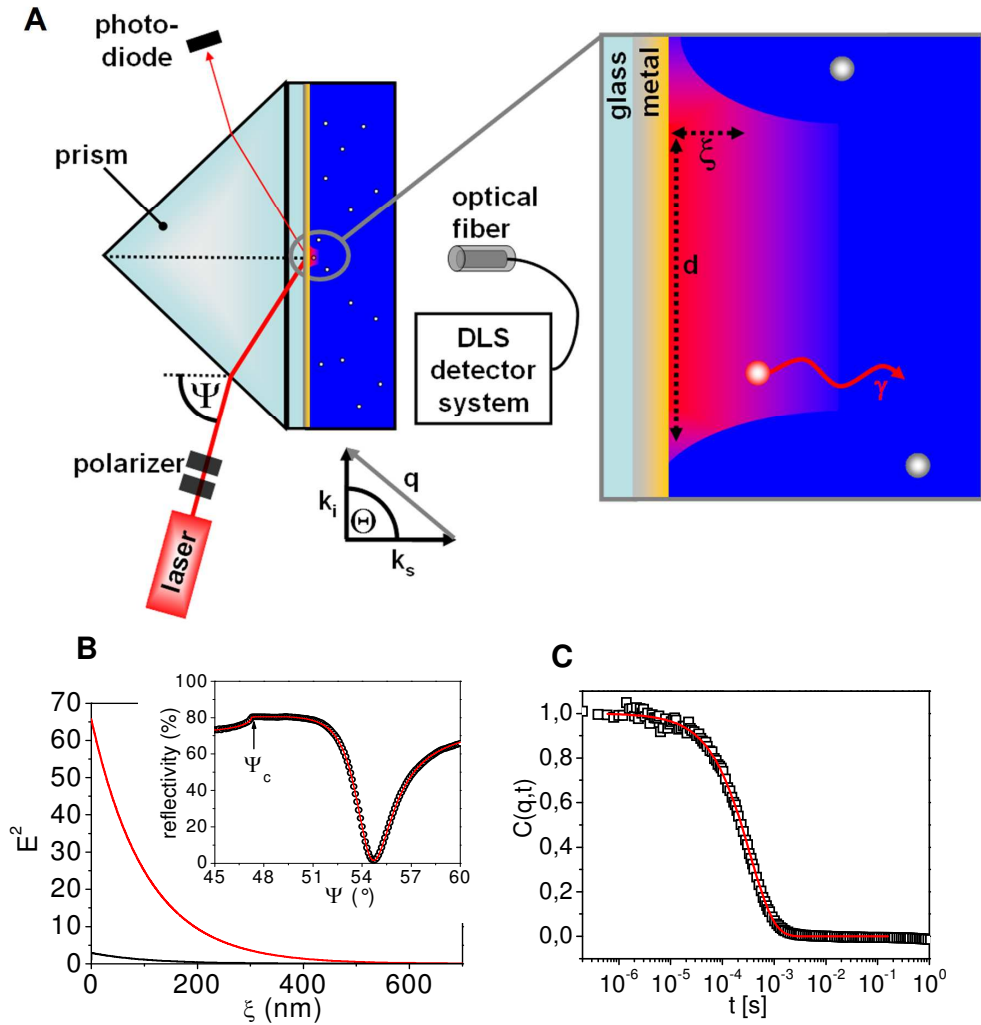


Fig. 1. (A) The REDLS-Setup is a standard Kretschmann-Raether configuration (p-polarized light at an incidence angle Ψ) of a SPR combined with a DLS technique to record the intensity correlation function at an angle Θ defining the scattering vector $\mathbf{q}=\mathbf{k}_s-\mathbf{k}_i$ with \mathbf{k}_i and \mathbf{k}_s being the wave vectors of the evanescent and scattered electric field. The enlarged region in the middle cartoons the scattering volume with the electromagnetic field of the surface plasmon, its penetration depth ($\xi=200\text{nm}$) and its footprint ($d\approx 200\mu\text{m}$). Only particles within the evanescent field contribute to the scattered light (γ). The condition for surface plasmon excitation by light is given by Eq. (1). (B) Field enhancement in the SPR (red line) compared to total internal reflection (black line). A reflection curve of a surface plasmon with Ψ_c being the total internal reflection angle is shown in the inset. (C) Normalized field-autocorrelation-function $C(q,t)$ for polystyrene latex spheres with radius $R=30\text{nm}$ and $c=0.56\text{g/l}$ at a scattering angle $\Theta=112^\circ$ ($q=0.022\text{nm}^{-1}$) represented by an exponential decay function (solid line).

where k_i is the wavevector of the surface plasmon [17] and the scattering angle Θ is obtained from the angle Θ' of the DLS detector taking into account the refraction at the water/quartz/air interfaces. This assembly is depicted in Fig. 1(A).

A LaSFN9 glass substrate covered with 35nm silver plus a 10nm gold layer by thermal evaporation was index-matched (immersion oil) to the base of a LaSFN9 prism; the thin gold layer prevents the oxidation of silver. Monochromatic light (HeNe-Laser, $\lambda=632.8\text{nm}$) with

linear, transverse magnetic polarisation is focused by means of a lens ($f=500\text{mm}$) onto the metal layer of a custom made cell, which is mounted on a two circle goniometer system.

Varying the external angle of incidence ψ , angle dependent intensities are recorded by a photo-diode. Figure 1(B) shows a transfer matrix calculation of the field enhancement factor [23] of about 60 based on the parameters extracted from the angle dependent reflectivity of the prism base (inset to Fig. 1(B)) using WINSPALL 3.01 [24].

The electromagnetic field of the surface plasmon is utilized as the incident beam of the DLS experiment. The correlation function $C(q,t)$ (Fig. 1(C)) is recorded by the DLS detector system consisting of a lens, that focuses the scattered light onto a single mode fibre, an avalanche photodiode, and an ALV5000 digital multiple tau correlator. The aqueous dispersion of the particles was filtered into a quartz crystal cell (volume $\sim 20\mu\text{l}$) to ensure easy cleaning and easy replacement of samples. The scattering volume can be approximated by a cylinder with a diameter $d=200\mu\text{m}$ and height equal to the surface plasmon penetration depth $\xi=0.2\mu\text{m}$ estimated from the exponential decay of the electric field (the distance from the interface at which the amplitude of the field falls to $1/e$ of its value at the metal surface) [16]. A direct comparison between REDLS and EWDLS was performed at a scattering angle $\Theta=90^\circ$ for polystyrene (PS) latex particles with $R=20\text{nm}$ and $c=0.9\text{g/l}$ using 1mW laser power. REDLS led to a good quality $C(q,t)$ equal to the statistics of Fig. 2(B), whereas in the EWDLS geometry a correlation function could hardly be detected in the data. This confirms the enhanced light scattering from a sphere of 100nm radius placed in the optical field of the SPR [25].

4. Results

4.1. Surface correlation functions obtained by REDLS

Figure 2(A) shows surface correlation functions decaying over five orders of magnitude in time for a dilute aqueous solution of PS spheres with $R=30\text{nm}$ at three different scattering angles in

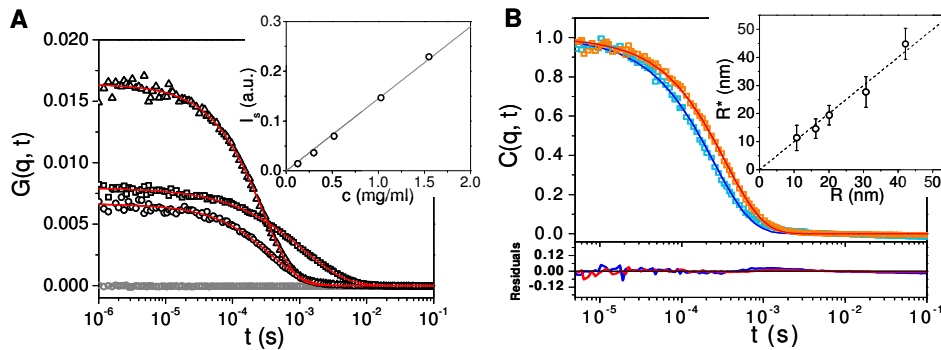


Fig. 2. Time correlation functions for particle diffusion near a gold surface obtained by REDLS. (A) Correlation functions $G(q,t)$ for dilute solution of polystyrene spheres ($c=0.56\text{g/l}$ with $R=30\text{nm}$ at various scattering angles (square: $\Theta=54.8^\circ$, $q=0.012\text{nm}^{-1}$; triangle: $\Theta=90^\circ$, $q=0.019\text{nm}^{-1}$; circle: $\Theta=125.2^\circ$, $q=0.023\text{nm}^{-1}$) represented (solid lines) by the stretched exponential function [Eq. (3)]. The deviation from the single exponential shape is more pronounced at low scattering angles. The correlation function for pure water recorded at $q=0.019\text{nm}^{-1}$ is a flat base line (gray circles). The scattering intensity ($q=0.019\text{nm}^{-1}$) from the particles (given by the product of the total scattering intensity from the solution in the illuminated volume in Fig. 1(A) and the short time plateau value $G(q,0)$) is a linear function of the particle concentration in dilute solutions as it is depicted in the inset. (B) Normalized correlation functions $C(q,t)$ for dilute solutions of PS with $R=20\text{nm}$ ($c=0.9\text{g/l}$, blue symbols) and $R=30\text{nm}$ ($c=0.56\text{g/l}$, red symbols) at $q=0.022\text{nm}^{-1}$ represented well (deviation plot) by an exponential shape. The inset shows a comparison between the values of the particle radius R^* obtained by REDLS at $q=0.019\text{nm}^{-1}$ (open circles) and conventional DLS in the bulk dilute solutions (dashed line).

the q range 0.012nm^{-1} to 0.023nm^{-1} .

Firstly four crucial tests of the validity of the new experimental technique are worth mentioning: A flat baseline-like $G(q,t)$ was found for pure water as seen in Fig. 2(A), a low value of $G(q,t)$ at short times due to the heterodyning detection, the linear increase of the scattering intensity I_s (inset of Fig. 2(A)) with the particle concentration c in the dilute regime and the slowing down of $C(q,t)$ with particle size (Fig. 2(B)). Note that I_s is estimated from the product of the contrast $G(q,t=0)$ times the total scattering intensity measured at the DLS detector (Fig. 1(A)) comprised of the quasielastic and the elastic scattered light. The experimental $G(q,t)$ assumes almost an exponential decay that is very well represented by a stretched exponential function with the exponent $0.85 < \beta < 1$ as seen in the residual plot of Fig. 2(B). At lower q values, $G(q,t)$ displays larger deviations from a single exponential shape and the value of the exponent β varies between $0.65 < \beta < 0.85$; the surface plasmon penetration depth becomes relevant at low q 's as $q\xi \leq 1$. In the bulk, the recorded $C(q,t)$ of the same dilute dispersion is single exponential ($\beta \approx 1$) as expected for these almost monodisperse particles. The existence of the solid surface and the presence of the two length scales, ξ and q^{-1} renders deviations of the surface $C(q,t)$ from the bulk correlation function conceivable. In addition to the topological i.e.: mirror effect, finite scattering volume and physical effects i.e. anisotropic diffusion [5,9], surface modifications i.e. adsorption, chemical reactions might also occur. An important advantage of the present REDLS technique is the sensitivity of SPR on solute induced surface modifications. No shift in the SPR angle (inset to Fig. 1(B)) was detected during the REDLS experiment. Thus we can exclude any alteration of the surface as well as partial adsorption of the particles.

4.2. Q -dependency

Information on surface-induced hindered diffusion and anisotropy of Brownian motion can be extracted from the q -dependence of the characteristic relaxation rate $\Gamma(q)$ of the experimental $C(q,t)$. For free particle diffusion in dilute bulk solutions, $C(q,t)$ is a single exponential function (dashed lines in Figs. 3(A), 3(B)); For the particle diffusion near the gold surface, the

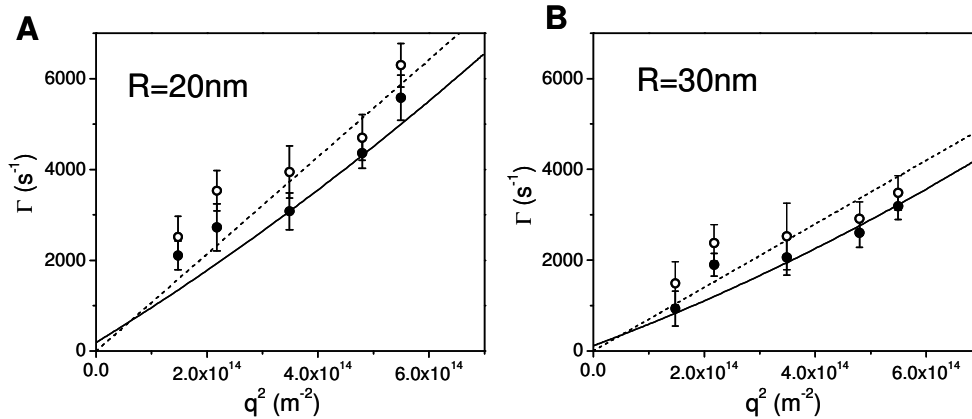


Fig. 3. Particle diffusion at a water/gold interface. The variation of the relaxation rate Γ obtained either from the initial slope (Γ_c , open symbols) or from integral (Γ_{av} , solid symbols) of the time correlation functions (Fig. 2) for particle Brownian motion near the gold surface at a penetration depth $\xi=200\text{nm}$ with the magnitude of the scattering wave vector q . The dashed line indicates $\Gamma_0=D_0q^2$ for the free Brownian motion of the PS particles ((A) $R=20\text{nm}$, $c=0.9\text{g/l}$ and (B) $R=30\text{nm}$, $c=0.56\text{g/l}$) in the bulk solution as obtained by the conventional DLS. The confined Brownian motion near the gold surface is modelled by a hindered anisotropic diffusion (eq.5) using $D_{\perp}/D_0=0.65$ (for $R=30\text{nm}$) and $D_{\perp}/D_0=0.70$ (for $R=20\text{nm}$) and $D_{\parallel}/D_0=0.85$ (cp. Fig. 4 of reference [9]).

trend of the average $\Gamma_{av}(q)$ (solid points in Fig. 3) clearly deviates from the purely diffusive (D_0q^2) behavior in the bulk solution. Using the theoretical predictions [9] for $D_{||,\perp}/D_0$, Eq. (5) rationalizes (solid lines) the finite intercept (at $q=0$) and the deviation from the linear q^2 dependence of the experimental $\Gamma_c(q)$ (open symbols) for the two particles in Fig. 3. Remarkably at $q \approx 0.019 \text{ nm}^{-1}$ Γ_c falls very close to the free diffusion (dashed line in Fig. 3) and it is this range at which the nominal value of the radius compares well (inset to Fig. 2(B)) to the particle radius.

The results in Fig. 3 emphasize the importance of the q -dependent measurements in the study of dynamics near solid surfaces.

5. Conclusion and outlook

We have demonstrated the usability of a novel combination of SPR with DLS that allows for the probing of dynamic phenomena near metallic surfaces over broad time scales with sub micrometre spatial resolution. For the demonstration case of particle diffusion in the liquid-gold interface, the high quality relaxation functions reveal the surface-induced diffusion anisotropy in particular for the normal direction probed at lower scattering angles. The "classical" use of SPR in bio-affinity studies can now be complemented by this novel yet complementary tool for the dynamic evaluation of surface processes like the (constrained) diffusion of the analytes to the sensor-surface attached binding site.

Finally, it is worth mentioning the possibility of tuning the range of the evanescent field that probes the dynamics of the interface by using the optical field of two coupled surface plasmon modes propagating along a very thin metal layer in contact to the dielectric media of (nearly) identical refractive index one can either extend the range of the probing electromagnetic field to micrometers by employing the long range surface plasmon mode, or one can reduce the exponential decay of the evanescent wave to a range of a few tens of nanometers by using the short range component of the two new Eigenmodes of coupled surface plasmons [14,26].

Acknowledgments

We acknowledge A. Gerstenberg for technical support and M. Kreiter and A. Unger for help with theory and simulations as well as the EU (CP-FP-213948-2) for partial financial support. We thank Prof. J. Dhont and Dr. B. Loppinet for fruitful discussions.